Test Results of Sintered Nano-Silver Paste Die Attach for High Temperature Applications

Paul Croteau[1], Sayan Seal[2], Ryan Witherell[1], Michael Glover[2], Shashank Krishnamurthy[1], Alan Mantooth[2]

[1] United Technologies Research Center
411 Silver Lane, East Hartford, CT, 06118
croteapf@utrc.utc.com

[2] University of Arkansas, High Density Electronics Center (HiDEC), 700 Research Center Blvd, Fayetteville, AR 72701

Abstract

The emergence of wide band gap devices has pushed the boundaries of power converter operations and high power density applications. It is desirable to operate a power inverter at high switching frequencies to reduce passive filter weight and at high temperature to reduce the cooling system requirement. Therefore, materials and components that are reliable at temperatures ranging from -55 to 200 °C, or higher, are needed. Sintered silver is receiving significant attention in the power electronic industry. The porous nature of sintered nano-silver paste with a reduced elastic modulus has the potential to provide strain relief between the die component and substrate while maintaining its relatively high melting point after sintering. The test results presented herein include tensile testing to rupture of sintered silver film to characterize stress strain behavior, as well as die shear and thermal cyclic tests of sintered silver bonded silicon die specimens to copper substrates to determine shear strength and reliability.

Keywords
« Sintered silver », « nano-silver paste », « die attach », « high temperature », « temperature dependence », « material behavior », « shear strength »

1 Introduction

Sintered nano-sliver paste has received much attention for its potential to provide a reliable bond for electronic die components used at extreme temperature ranges of -55 to 200 °C or higher. Sintering of nano-silver particles occurs at a temperature of about 260 to 300 °C, with or without additional applied pressure. The sintered silver, although porous, is pure and maintains its bulk melting point of 962 °C. The porous nature of sintered silver, with a typical porosity of about 10-30%, produces a reduced modulus of elasticity that has potential as a strain relief between the ceramic die component and substrate.

The strength and fatigue material behavior of sintered silver was investigated extensively by Wang [1] by performing monotonic and cyclic uniaxial tensile tests at various temperatures and stress rates on thin 80 µm sintered silver specimens. Wang [1] demonstrated that sintered silver is very temperature and stress rate dependent, where the tensile strength of 45 MPa at room temperature decreased by approximately 50% when tested at 175 °C, and decreased by nearly 67% when tested at a slow stress rate of 1 MPa/min as compared to 100 MPa/min. Similarly, uniaxial ratcheting tests indicated a decrease in cyclic life when exposed to increased temperature and decreased stress rate.

The use of sintered silver as a method for die attachment for use in high temperature applications has also been investigated for strength and reliability against fatigue. Bai [2] showed that the dwell time at the sintering temperature significantly effects the bonding and shear strength of the sintered silver die attach, with a maximum shear strength of 40 MPa achieved after a 40 minute dwell at sintering temperature of 300°C. Additionally, Bai [2] performed thermal cycle testing between 50 °C and 250 °C on small 1.7 mm x 1.4 mm silicon devices bonded to various substrates, showing a 50% drop in shear strength for bonds to a Al_2O_2 substrate after 4000 cycles, and a similar drop in strength for bonds to copper substrates after 500 cycles.

The failure mechanism associated with thermal cycling is attributed to the high stress and strain imparted on the die attachment caused by the CTE mismatch between the die and substrate materials. Understanding the fatigue behavior of the die attach material is critical for predicting and designing for required life and reliability. Chen [3] performed cyclic shear tests on specimens of 5 mm x 5 mm chips attached to copper substrates with a

50 μm of sintered silver in effort to characterize the ratcheting behavior of the die attach. Chen [3] compared actual experimental data with results from two viscoplasticity material models by Anand and by Ohno-Wang & Armstrong-Frederick (OW-AF). Chen [3] showed that the test results of accumulated plastic strain from cyclic shear loading agreed better with the OW-AF kinematic hardening model than with the Anand model, where the Anand model tends to overestimate the cyclic plastic strain.

The magnitude of stress and strain during a thermal cycle depends not only on the particular CTE mismatch as explored by Chen [3], but also on matters of the design of the component, such as selection of substrate material, size of the die, thickness of the sintered silver bond line, and the sintering process itself. Since the driving force behind most failures of any die attach is thermal strain due to CTE mismatch between the die and substrate, selection of a substrate with an effective CTE that matches as closely as possible the CTE of the die material will minimize cyclic thermal strain. Additionally, a larger die footprint leads to higher shear stress of the die attach material along the edge and corners of the die. The thickness of the bond line affects the stress-strain in the die attach bond line, increasing as the bond line thickness decreases. Also, the sintering process not only affects the quality of the bond to the metalized surfaces of the die and substrate, but also will determine the amount and location of the porosity; this can affect the initiation and progression of cracks in the sintered silver bond line.

The motivation for the work described in this paper was to characterize the tensile and shear strength of sintered nano-silver as well as its plastic strain behavior due to thermal cycling. As such, the test results presented herein include tensile testing to rupture of sintered silver film, die shear testing of silicon dies bonded with sintered silver die attach, and thermal cycle testing square silicon dies sintered to copper substrates. All specimens were fabricated by our project partners at the University of Arkansas (UARK). The nano-silver paste used for fabrication of these test specimens was NanoTach®-X from NBE Tech, Blacksburg, VA.

Tensile rupture tests of sintered silver film with thickness ranging from 80 to 100 μm were performed at various strain and stress rates and at various elevated temperatures. Typical rupture strengths were 30 to 35 MPa at ambient temperature and 10 MPa at 200 °C. The tensile testing was also performed to obtain elastoplastic stress-strain behavior needed for parameter calculations for future material modeling based on Kang's [4] time-dependent constitutive model variation of the Abdel-Karim and Ohno [5] kinematic hardening model.

Die shear tests were performed prior to thermal cycling tests at various temperatures to obtain baseline shear strengths as a function of temperature and bond line thicknesses. Shear strengths for 50 to 120 μm thick bond lines were approximately 35 to 40 MPa at ambient temperature with a sharp decrease to 20 MPa for a 2 0μm bond line.

Accelerated life testing was performed by thermal cyclic testing on a number of highly CTE mismatched silicon-to-copper specimens. Variations of bond line thickness (50 to 120 μm), die size (2 mm and 4 mm square), and temperature range (-40 to 150 °C and -50 to 200 °C) were investigated. Life was negatively impacted with increased die size and decreased bond line thickness. Crack formation and propagation were observed and documented through SEM imaging of samples at regular intervals.

2 Test Articles

2.1 Uniaxial Tensile Specimens

Film-like uniaxial tensile specimens were fabricated by performing two consecutive stenciling and sintering operations onto an alumina substrate. A 100 μm (4 mil) thick Mylar stencil was cut for (12) 25 mm x 3 mm tensile specimens. The NanoTach®-X nano-silver paste obtained from NBE Tech, LLC, in Blacksburg, VA, has a solid loading of approximately 88% with a silver particle size distribution of 50 nm to 7 μm. The paste was applied and squeegeed onto the stencil cutouts. The wet paste was dried and sintered with the combined temperature profile as shown in Figure 1. A second stenciling application with the same 4 mil stencil was squeegeed on top of the now sintered layer and dried and sintered with the same temperature profile in Figure 1.

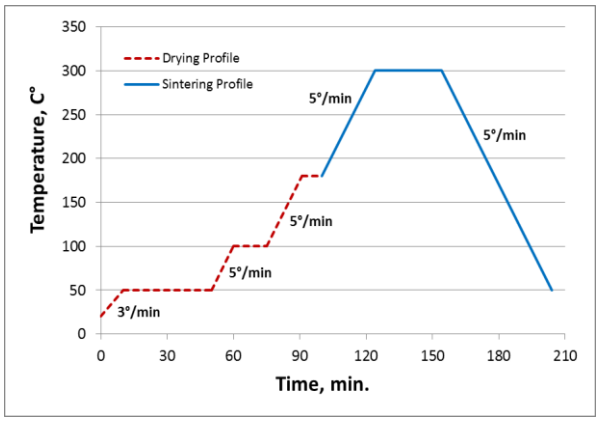

Figure 1: Sintering temperature profile for uniaxial tensile specimens.

The drying and sintering operations as defined above were performed using a Fisher Scientific Isotemp series oven. The oven environment was ambient air with no assisted airflow.

To remove the tensile specimens from the alumina substrate, as shown in Figure 2, the specimens were first immersed into a dilute 0.01% hydrochloric acid (HCl) and then lifted carefully lifted from the substrate with a razor. The tensile specimens were analyzed for thickness, surface profile, and porosity. A Dektak profilometer was used to measure its thickness across the 3 mm width of several specimens. Figure 3 illustrates a typical result from the profilometry, indicating a specimen thickness of approximately 100 μm with an occasionally small increase of thickness at the edges, an artifact of the stenciling operation.

Figure 2: Uniaxial test specimens, (12) 25mm x 3mm x 100μm thick specimens sintered on Al_2O_3 substrate.

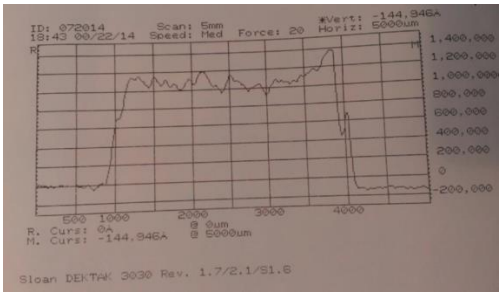

Figure 3: Typical thickness profile of uniaxial tensile specimens as measured by Dektak profilometer.

A small number of specimens were mounted, sectioned and polished for SEM imaging. Figure 4 illustrates a typical cross section of the sintered silver tensile specimens. The distribution of porosity was fairly even and consistent throughout and was determined to be approximately 30% porosity, toward the upper bound of what is specified in the NBE Tech product data sheet.

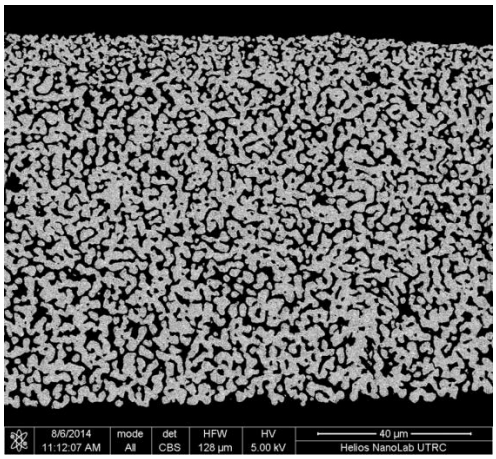

Figure 4: SEM cross sectional image of sintered silver uniaxial test specimen, approx. 30% porosity.

2.2 Die Shear and Thermal Cyclic Test Specimens

The fabrication process for the die shear and thermal cycling test specimens required bonding square silicon die pieces to pure copper substrate using a variation of the drying and sintering process described in the previous section. Copper was used as the substrate material to provide a large CTE mismatch with the silicon, thereby accelerating the failure of the bond.

The copper substrate required a metallization of the surface with either gold or silver for adhesion of the sintered silver to occur. Bai [2] investigated the shear strength of sintered silver using both gold and silver metallization and showed improved shear strength performance with silver. Therefore, a process was developed where a 0.80 μm thick nickel layer was first electroplated to the copper. The nickel was needed to provide adhesion of the subsequent silver layer as well as acting as a diffusion barrier, preventing diffusion of the silver into the substrate. A very thin layer of silver 100-200 nm thick was then applied by silver strike method, which demonstrated good adhesion to the nickel and served to passivate the nickel layer. The final layer of silver was electroplated to the silver strike to a thickness of about 0.4 μm. Table 1 below outlines the plating process in more detail. Figure 5 illustrates the final silver plated copper sheet ready for dicing and bonding with the silicon die pieces.

A 127 mm (5 in) diameter x 0.675 mm thick silicon wafer was used for the die material. The silicon wafer had a single polished side onto which a 0.05 μm layer of titanium followed by a 2 μm layer of copper was applied by sputtering. The wafer was photo-lithographically patterned into what would become the 2 mm x 2 mm die needed for die attachment. The electroplating of nickel

and silver onto the wafer's die pattern followed a very similar process as the substrate with a small change in final silver electroplating time. Table 2 outlines the details of the electroplating process for the silicon die wafer. Figure 6 illustrates the resulting electroplated silicon wafer with the 2 mm x 2 mm die pattern clearly visible.

The development of a successful sintered silver bond line with a consistent and even distribution of porosity in the range of 10-30% for various bond line thicknesses required several iterations. The sintering temperature and time recommended by NBE Tech was a maximum temperature of 260 °C for 30 minutes for bond line thickness between 15 to 30 μm. Additionally, application of a pressure load was not required for small die pieces less than 10 mm x 10 mm.

Table 1: Electroplating process for copper substrate

Plating Mat'l	Current (mA)	Time (minutes)	Thickness (nm)
Nickel	0.25	10	800
Silver Strike	0.1	1	100-200
Silver	0.1	10	400

Table 2: Electroplating process for silicon die wafer

Plating Mat'l	Current (mA)	Time (minutes)	Thickness (nm)
Nickel	0.25	10	800
Silver Strike	0.1	1	100-200
Silver	0.1	5	400

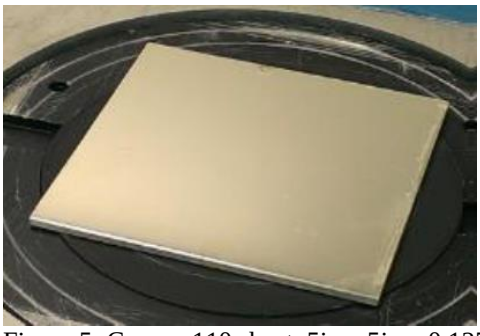

Figure 5: Copper 110 sheet, 5in x 5in x 0.125in, with final electroplated silver.

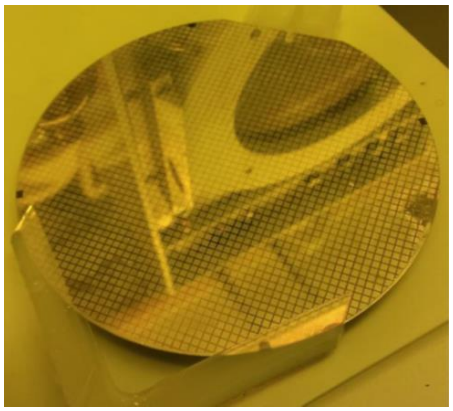

Figure 6: Silicon Wafer, 5 inch diameter, patterned and electroplated.

Initial trials indicated that porosity was sensitive to sintering temperature and time, as well to the bond line thickness. Although the manufacturer's recommended sintering temperature is 260 °C, the initial trials were sintered at the same 300 °C used for the uniaxial tensile specimens. The result was a bond line that was mostly of very low porosity sintered material as illustrated in Figure 7, or with variable porosity as illustrated in Figure 8. A lower sintering temperature was subsequently used to attempt to achieve a higher porosity and more even distribution of porosity. A fourth iteration involved 1) applying the silver paste by stencil, 2) drying each stenciled layer (if more than one was to be applied), 3) applying a dot of wet paste to the die surface, 4) mounting to dried paste surface and 5) sintering. This produced a sintered silver bond line that was free of major voids or cracks and had porosity in the desired 10-30% range. That variation continued to be seen within the same bond lines, as shown in Figure 9, where the two SEM images are from the same die bond line cross section.

A final process was defined using a sintering temperature of 270 °C that achieved three bond line thicknesses required for testing and had an adequate amount and distribution of porosity. For die attachments with multiple applications of silver paste, a drying of the paste was required after the first application of paste using the temperature profile in Figure 9. The sintering profile used includes a drying phase prior to ramping to the sintering temperature as shown in Figure 10. The dwell at 180 °C during the drying phase previously used for the uniaxial tensile specimens was eliminated based on further recommendations from NBE Tech, indicating that the organics outgassing during the ramp up to 270 °C was sufficient and a dwell at 180 °C was not necessary.

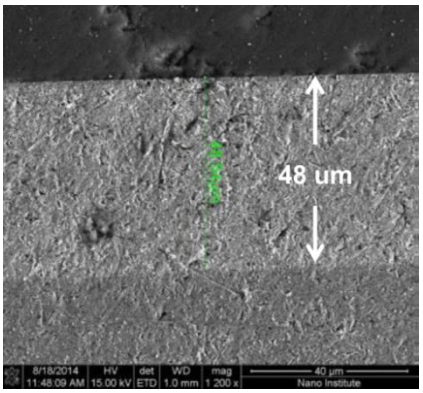

Figure 7: SEM image of sintered silver from die attach Iteration 1 showing very low porosity.

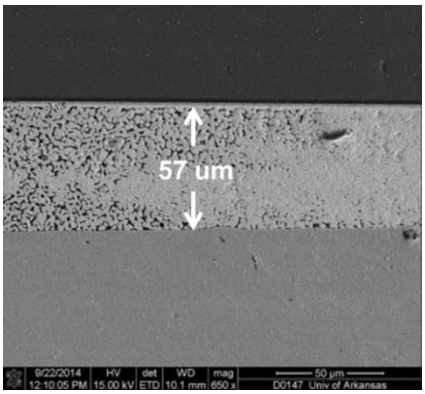

Figure 8: SEM image of sintered silver from die attach Iteration 3 showing variable porosity.

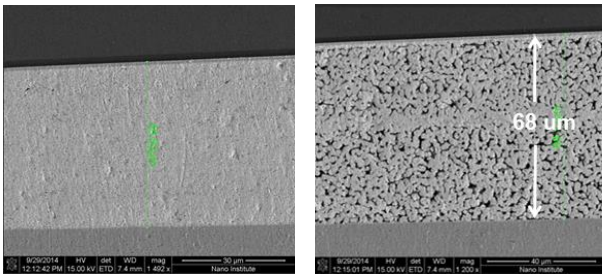

Figure 9: SEM image of sintered silver from die attach Iteration 4 showing variable porosity.

The final procedures defined for a varying die attachment bond line thickness were as follows:

1) For a 25 to 30 µm bond line, 50 µm wet paste was stenciled onto the substrate with a 50 µm (2 mil) stencil, followed by applying the 2 mm die into the wet paste with light downward pressure and twisting motion (termed here as "scrubbing") to ensure wetting to the die surface. Sintering was then performed at 270 °C for 30 minutes, using the temperature profile shown in Figure 11.

2) For a 50 to 60 µm bond line, 50 µm wet paste was stenciled onto the substrate with a 50 µm (2 mil) stencil and dried at 100 °C using the profile in Figure 10. A dot of wet paste was applied onto the 2 mm die and it was then scrubbed into the dried paste to ensure wetting of both surfaces. Sintering was then performed at 270 °C for 30 minute using the temperature profile in Figure 11.

3) For a 70 to 90 µm bond line, 75 µm wet paste was stenciled onto the substrate with a 75 µm (3 mil) stencil and dried at 100 °C using the profile in Figure 10. A second 75 µm layer of wet paste was applied on top of the dried paste using the same 75 µm stencil and another drying step was performed. A dot of paste was then applied onto the 2 mm die and the die was scrubbed into the dried paste to ensure wetting of both surfaces. Sintering was performed at 270 °C for 30 minutes, using the temperature profile shown in Figure 11.

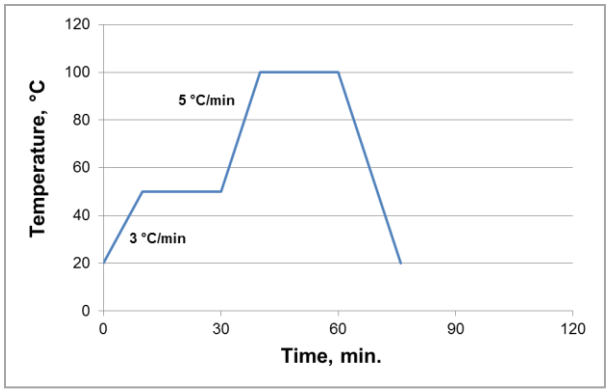

Figure 10: Drying profile for die attach with multiple layers of silver paste.

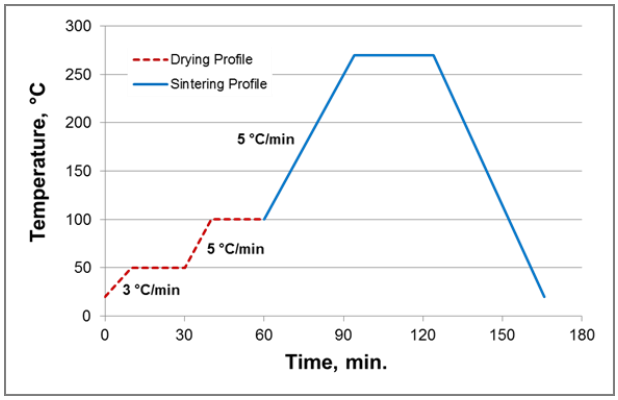

Figure 11: Sintering profile for die attach with single layer of silver paste.

3 Discussion of Test Results

3.1 Uniaxial Tensile Test

Tensile testing of the film-like sintered silver specimens was performed on a TA Instruments Q800 Dynamic Material Analyzer, or DMA. Tensile specimens were tested at various temperature, stress rates, and strain rates as outlined in the test matrix below in Table 3.

Figure 12 shows a definite effect of temperature on the stress-strain behavior of the sintered silver, where all tensile specimens were tested under stress rate control at 100 MPa/min and at temperatures ranging from -55 °C to 200 °C. As expected, as the temperatures increase, there was a corresponding decrease of elastic modulus and tensile strength and a decrease of elongation. Assuming ambient condition as the baseline, the change in the instantaneous elastic modulus was about 0.26% per °C between -55 °C and 100 °C and increasing a little to about 0.33% per °C between 175 °C and 200 °C.

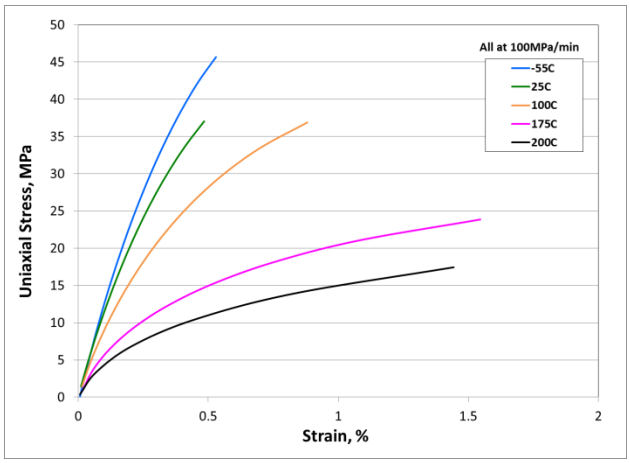

Figure 12: Stress-strain curves for sintered silver illustrating temperature at a stress rate of 100 MPa/min.

Figure 13 illustrates the stress-strain behavior at lower stress rates, 10 and 1 MPa/min as compared to 100 MPa/min. At an ambient temperature of 25 °C, there was little effect of the moderate stress rate of 10 MPa/min as compared to faster 100 MPa/min, but the material begins to show a reduced modulus and reduced tensile strength at the even slower stress rate of 1 MPa/min. The effect of an elevated temperature of 175 °C on the material was apparent at all stress rates, with a much reduced elastic modulus and tensile strength with an increased elongation.

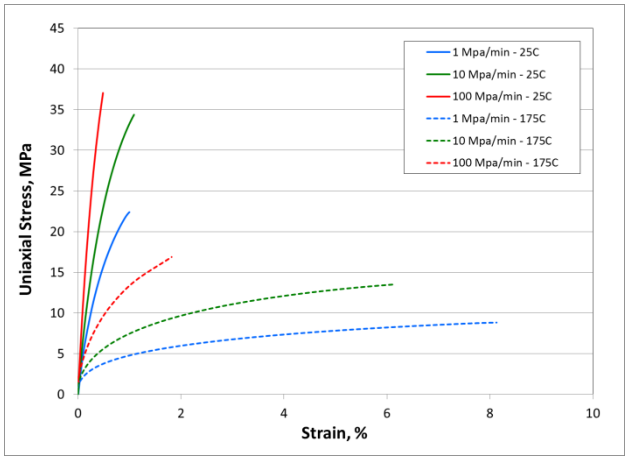

Figure 13: Stress-strain curves for sintered silver illustrating temperature and stress rate dependency.

The combined effect of increased temperature and reduced stress rate on tensile strength was dramatic, decreasing approximately 50% for each stress rate with a an increase of temperature form 25 °C to 175 °C, with a corresponding increase of elongation of 4 to 8 times.

Table 3: Uniaxial Tensile Test Matrix for Sintered Silver Tensile Specimens

Test	Effect of temperature	Effect of stress rate	Effect of strain rate
Specimen Size	25 mm x 3 mm x 80 um		
Temperatures	-55 °C, 25 °C, 100 °C, 175 °C, 200 °C	20 °C, 175 °C	-55 °C, 25 °C, 100 °C, 150 °C, 175 °C, 200 °C
Stress or Strain Rate	1, 10, 100 MPa/min	1, 10, 100 MPa/min	0.0001, 0.01, 0.1 %/sec

Figures 14, 15 and 16 show the effect of temperature of the sintered silver tensile specimens when tested with strain rate control. Three strain rates, 0.1, 0.01, and 0.001% strain/sec were used at temperatures ranging from -55 to 200 °C. At the fastest applied strain rate of 0.1% strain/sec, the sintered silver demonstrated a steadily decreasing tensile strength with increasing temperature with little change in elongation, until for those specimens tested at 150 °C and above. The effect of elevated temperature progressed to lower temperatures as the strain rate decreased to 0.01 and 0.001% strain/sec. At 0.01% strain/sec and 100 °C, the tensile strength decreased by about 10% with a quadrupling of elongation to about 2% strain. The effect of decreased tensile strength and increase of strain elongation was even more pronounced at temperatures of 150 °C and above.

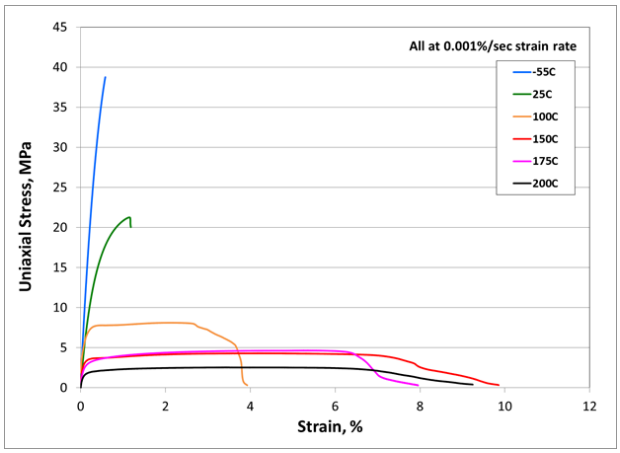

Figure 16: Stress-strain curves for sintered silver illustrating temperature at 0.001% strain/sec rate.

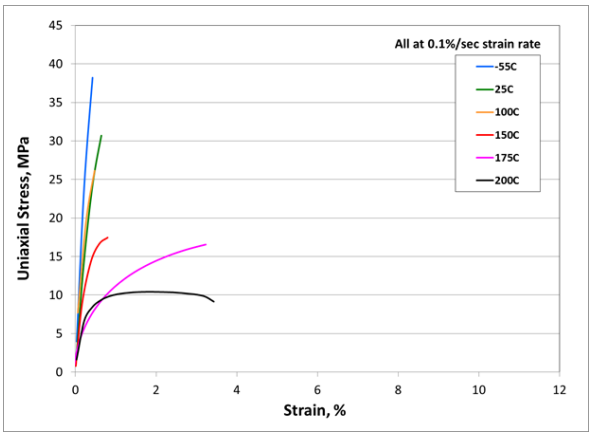

Figure 14: Stress-strain curves for sintered silver illustrating temperature at 0.1% per sec. strain rate.

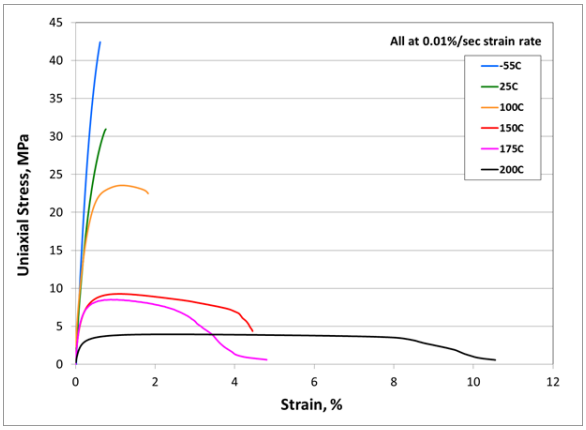

Figure 15: Stress-strain curves for sintered silver illustrating temperature at 0.01% per sec. strain rate.

The effect of further lowered strain rate was illustrated at 0.001% strain/sec in Figure 16, where the effect of the lower applied strain rate was evident even at the ambient temperature of 25 °C. At 100 °C, tensile strength decreased another 66% with a corresponding another doubling of elongation. The lower strain rate also showed significant impact at 150 °C and 175 °C, where the strengths and elongations were essentially equivalent to the results at 200 °C.

The tensile tests of the film-like sintered silver specimens were performed to characterize the stress-strain behavior over a large range of load and environmental conditions. Additionally, these tests provided the temperature dependent data required to develop the input parameters needed for an ANSYS material subroutine, or UserMat, that is being developed for simulating the ratcheting behavior of sintered silver die attachment during thermal cyclic loading. The ANSYS UserMat subroutine is based on work by Kang [4] and Abdel-Karim and Ohno [5]. Kang [4] developed a time-dependent constitutive model variation of the Abdel-Karim and Ohno [5] kinematic hardening model. Determination and usage of these parameters are beyond the scope of this discussion, but an example of the resulting model compared to test data is illustrated in Figure 17.

Briefly, a fourth order polynomial relationship was developed from test data of two uniaxial tensile tests performed at 0.01% strain/sec and 25 °C. The solid color lines in Figure 17 show different attempts at determining the material model parameters and the resulting stress-strain response from a simple ANSYS FEA model. The determination of the parameters is sensitive to the yield point chosen for the material as well as the divisions the stress strain curve will be segmented into, thereby

defining the number of parameters being calculated. That sensitivity is illustrated in the three response curves labeled Sintered Ag1, Sintered Ag3, and Sintered Ag7, and is compared to the response curve Sintered Ag_Chen, using parameters as determined by Chen [3]. The intent of this work will be to develop a temperature-dependent material model based on Kang [4] and Abdel-Karim and Ohno [5] using the test data obtained and presented in this paper.

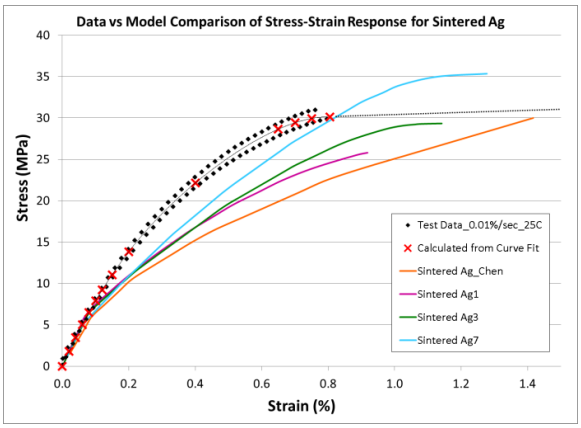

Figure 17: Stress-strain response curves for sintered silver, comparing AOK material model results with tensile test data at 0.01% per sec. at 25 °C.

3.2 Die Shear Testing

A small set of silicon-to-copper die attachments were fabricated with three varying bond line thicknesses of sintered silver; nominally 20 µm, 50 µm, and 120 µm. The specimens were tested for shear strength at temperatures of 25 °C, 150 °C, and 200 °C. The test was performed using a Nordson-Dage Series 4000 die shear tool. With the specimen mounted, a 5 mm flat die shear tip was positioned so as to apply load directly on the silicon die close to the sintered silver bond line. The three bar charts of Figure 18 illustrate the results of the die shear strength tests.

The 120 µm bond line specimens demonstrated a shear strength at a 25 °C ambient temperature of approximately 38 MPa, with essentially no reduction in shear strength at 150 °C and a small 4% reduction at 200 °C.

The 50 µm bond line specimens demonstrated a shear strength of approximately 35 MPa at 25 °C. The reduction of shear strength was relatively more pronounced at elevated temperatures, with a 34.2% decrease at 150 °C, and 8.4% decrease at 200 °C.

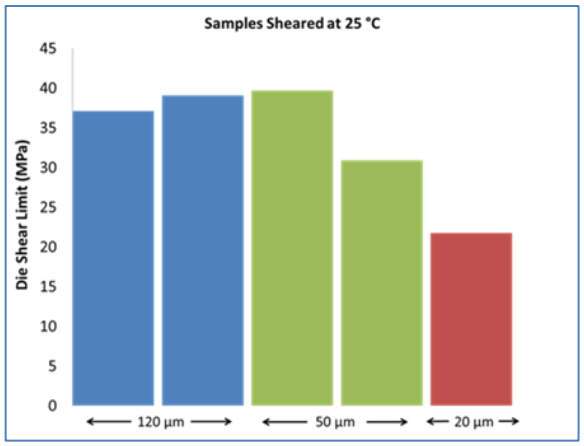

a) Die Shear results at 25 °C.

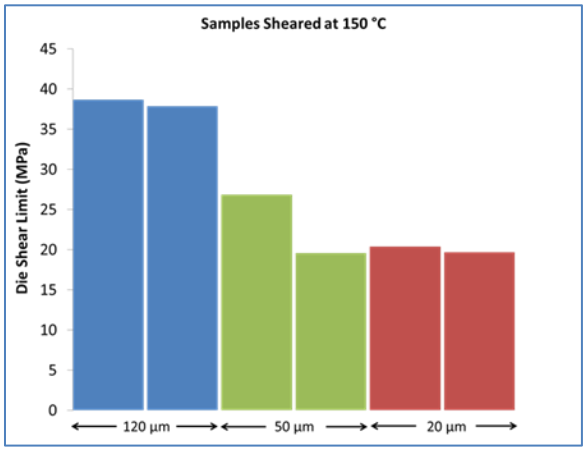

b) Die Shear results at 150 °C.

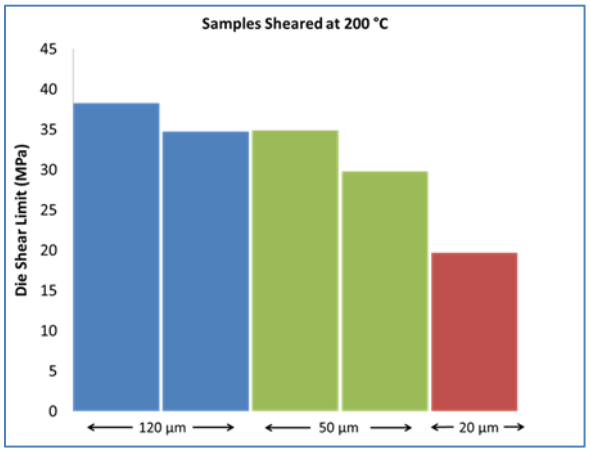

c) Die Shear results at 150°C.

Figure 18: Die shear results for sintered silver silicon die with 20 µm, 50 µm, and 120 µm bond line thicknesses at temperatures a) 25 °C, b) 150 °C, c) and 200 °C

Compared to the thicker bond line specimens, the 20 μm thick bond line showed a consistently low shear strength of approximately 20 MPa at 25 °C at all temperatures. The reduction of shear strength at 150 °C was approximately 8% and 10% at 200 °C.

3.3 Thermal Cycle Testing

The thermal cycling samples were divided into four separate lots, depending on die size, bond line thickness, and the temperature range of thermal cycling. Table 4 below provides a description of the four different lots based on these parameters. Lot1 served as the baseline with 2 mm x 2 mm die size and 50 μm bond line tested with a temperature range of -55 °C to 200 °C. A ramp-up and ramp-down rate of 10 °C/min with 10 minute dwell time at each temperature extreme was used for all four lots. Lot2 varied from Lot1 with a 120 μm bond line. Lot3 varied with a reduced temperature range of -40 °C to 150 °C. Lastly, Lot4 varied with a larger 4 mm x 4 mm die size. The testing was performed in a Delta 9023 Environmental Test Chamber, as shown in Figure 19, with a source of liquid nitrogen to provide the -55 °C temperature requirement.

Initially, NDE imaging using a scanning acoustic microscope, or SAM, was planned to determine the presence of cracks in the sintered silver bond lines or large scale delamination between the die and the substrate. This was to be validated with some destructive imaging using a scanning electron microscope, or SEM, of sectioned specimens.

The initial SAM images were not able to reliably capture clear images of the potential cracks or delaminations that were apparent in the SEM images. Therefore, the effect of damage due to crack propagation from thermal cycling was assessed using the destructive method of die shear strength and was not implemented until 175 and 200 cycles of Lot1 and Lot2, respectively, thereby missing some of the potential effects on shear strength from progressive damage that could have occurred prior to the 175 or 200 cycle interval.

The following discussion focuses on Figures 20, 22, 24 and 26, which outline the results of shear strength tests performed at various intervals throughout the thermal cycling tests on the four lots of specimens. Corresponding SEM images in Figures 21, 23, 25, and 27 illustrate the progression of damage at different intervals of the thermal cycling.

The initial shear strength testing of the baseline specimens of Lot1 (Figure 20) indicated a strength of approximately 35 MPa, but suffered essentially complete failure with about 5% shear strength remaining after only 175 thermal cycles between -55 °C and 200 °C. Figures 21a) and 21b) show a specimen from Lot1 after 100 cycles with some cracking near the die's edge and progressing under the die. Figures 21c) through 21f) show the progression and gap growth of crack under the die at 150 and 175 cycles. The extent of damage at 150 cycle interval was essentially the same as that at the 175 cycle interval and could be deemed "failed" as well.

The initial shear strength testing of the specimens of Lot2 (Figure 22) indicated a strength of approximately 38 MPa. With additional data points for Lot2, the trend of shear strength reduction appeared to be exponential in nature, with a decrease of 61% and 77% after 200 and 300 thermal cycles, respectively. Figure 23a) shows a specimen from Lot2 after 100 cycles with a crack starting near the die's edge, but there was no evidence of crack progression under the die (Figure 23b). Similar results were seen after 150 cycles as shown in Figures 23c and 23d. At 200 cycles, in addition to the corner crack in the sintered silver (Figure 23e), voids along the substrate can be seen coalescing together into a crack and was more widespread under the die (Figure 23f).

Table 3: Thermal Cycling Test Specimens

Lot	Die size	Bond line thickness	Temperature cycling range	Temperature ramp rate	Dwell time
	(mm)	(μm)	(°C)	(°C/ min)	(min)
1	2 x 2	50	-55 to 200	10	10
2	2 x 2	120	-55 to 200	10	10
3	2 x 2	50	-40 to 150	10	10
4	4 x 4	50	-55 to 200	10	10

Figure 19: Thermal Cycle Testing Apparatus.

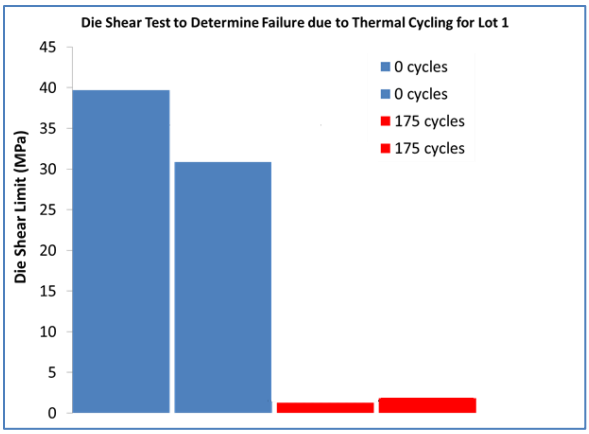

Figure 20: Lot1 Die Shear Results, 2 mm x 2 mm die, 50 µm bondline, and -55 to 200 °C range.

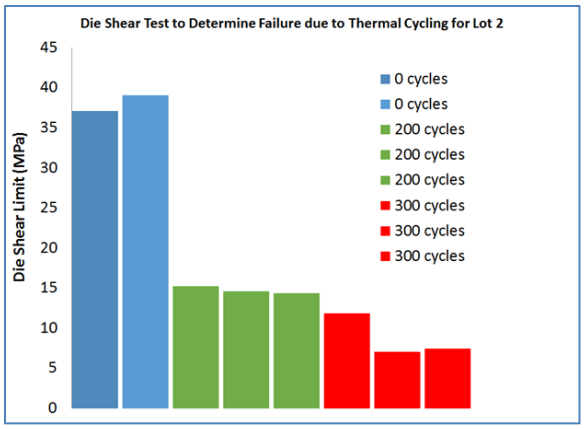

Figure 22: Lot2 Die Shear Results, 2 mm x 2 mm die, 120 µm bondline, and -55 to 200 °C range.

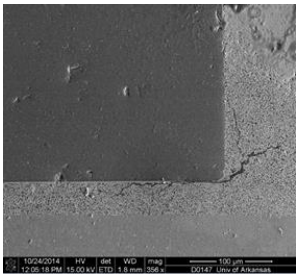

a) Corner crack in Ag at 100 cycles.

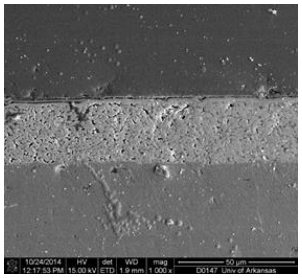

b) Crack in Ag under die at 100 cycles.

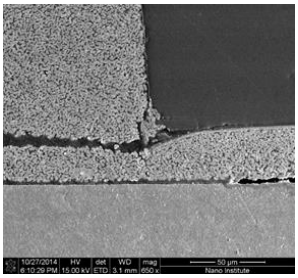

c) Corner crack in Ag at 150 cycles.

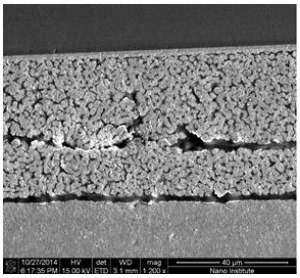

d) Crack in Ag under die at 150 cycles.

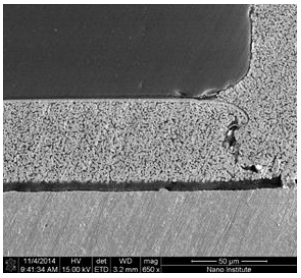

e) Corner crack in Ag at substrate at 175 cycles.

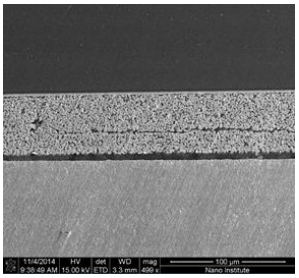

f) Crack in Ag at substrate at 175 cycles.

Figure 21: SEM Images of Lot1 specimens after 100, 150, and 175 cycles

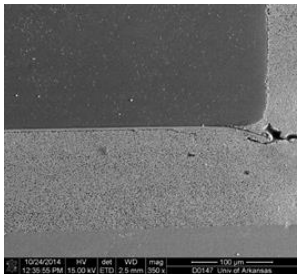

a) Corner crack in Ag at 100 cycles.

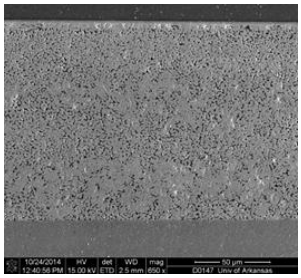

b) No damage under middle of die at 100 cycles.

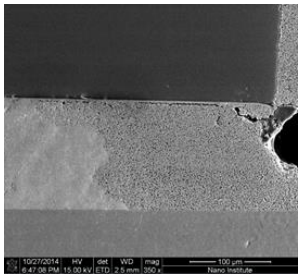

c) Corner crack in Ag at 150 cycles.

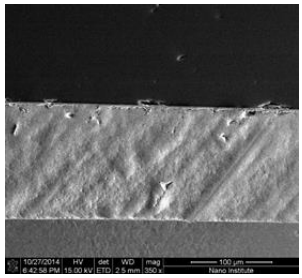

d) No damage under middle of die at 150 cycles.

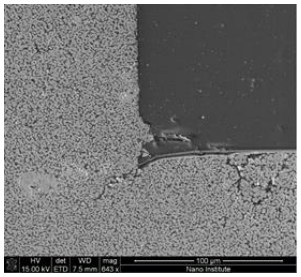

e) Corner cracking in Ag at 200 cycles.

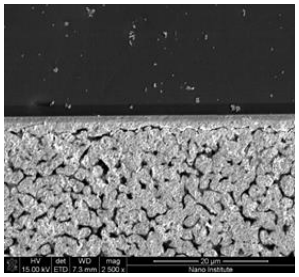

f) Widespread cracking under die at 200 cycles.

Figure 23: SEM Images of Lot2 specimens after 100, 150, and 200 cycles

Initial shear strength testing of the Lot3 specimens (Figure 24) indicated an initial strength of approximately 35MPa. Lot1 and Lot3 were from the same group of fabricated die specimens, with the temperature range used for thermal cycling reduced to -40 °C to 150 °C. As expected, the specimens of Lot3 performed better than Lot1, with a reduction of shear strength of 53%, 68%, and 78% after 100, 150, and 200 thermal cycles, respectively. SEM image of specimen from Lot3 (Figure 25a) after 50 cycles showed no evidence of crack at high magnification, but at lower magnification (Figure 25b), a dark line emerged that upon closer inspection was the start of coalescing voids. At 100 cycles, a corner crack was evident as was a fine crack extending into the silver under the die.

The low initial shear strength of 27 MPa for Lot3 (Figure 24) experienced a 71 % reduction only after 50 cycles, and remained essentially the same through 150 cycles. The early evidence of damage can be attributed to the increased thermal stress due to the larger die size.

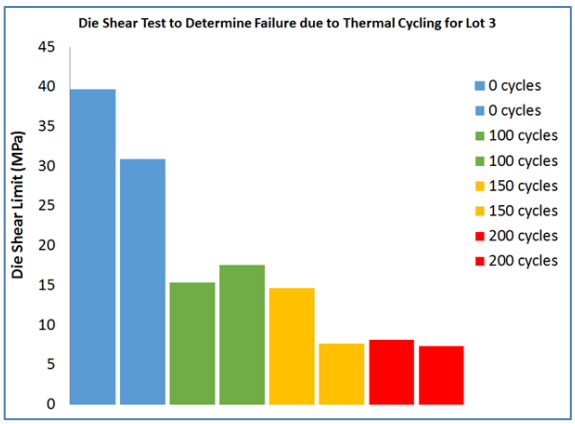

Figure 24: Lot 3 Die Shear Results, 2 mm x 2 mm die, 50 µm bondline, and -40 to 150 °C range.

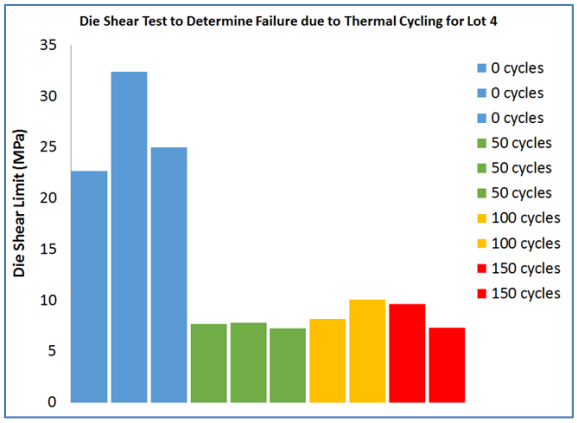

Figure 26: Lot 4 Die Shear Results, 4 mm x 4 mm die, 50 µm bondline, and -55 to 200 °C range.

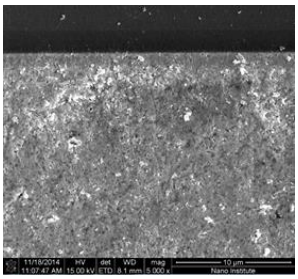

a) No detectable damage in Ag at 50 cycles.

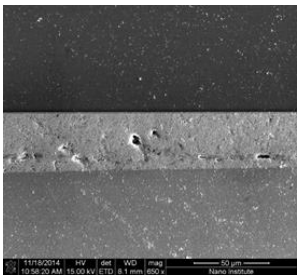

b) Coalescing voids at low magnification at 50 cycles.

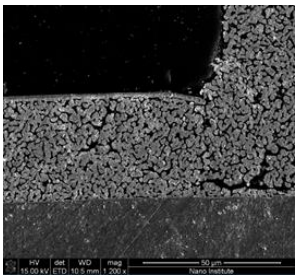

c) Corner crack in Ag at 100 cycles.

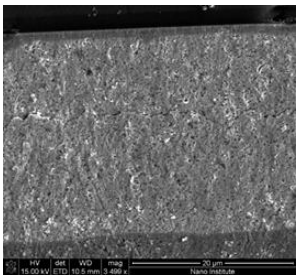

d) Crack in Ag under die at 100 cycles.

Figure 25: SEM Images of Lot 3 specimens after 50 and 100 cycles

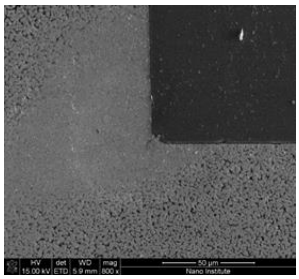

a) No detectable damage in Ag at 10 cycles.

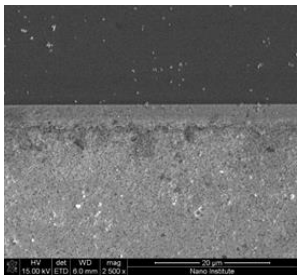

b) Some coalescing voids forming fine cracks.

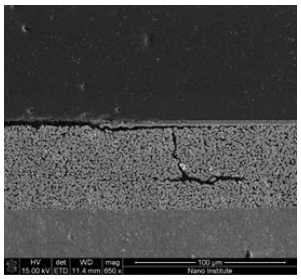

c) Crack extending in from corner at 50 cycles.

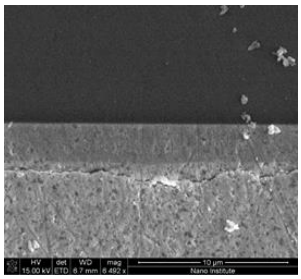

d) Crack in Ag under die at 50 cycles.

Figure 27: SEM Images of Lot 4 specimens after 10 and 50 cycles

4 Concluding Remarks

The tensile testing of the film-like specimens of sintered nano-silver paste provided useful temperature dependent and load rate dependent data. The tensile strength of the sintered silver agreed well with data from Wang [1], with a strength of about 35 MPa at 25 °C. More interestingly, there was a dramatic effect on elastic modulus, tensile strength, and elongation from the variation of stress rate and strain rate at various temperatures. Elevated temperature reduced tensile strengths by as much as 50% for a rise in temperature from 25 °C to 175 °C, with an eightfold increase in elongation. Furthermore, the temperature dependent stress-strain test results will provide the necessary data input for a visco-plastic material model based on Abdel-Karim and Ohno [5] and Kang [4] that will account for the behavior of sintered silver during thermal transients.

The results from the die shear tests illustrated that the sintered silver bond strength increased with increasing bond line thickness. The magnitude of shear strength did have a dependence on temperature. Specimens with thinner bond lines (50 µm and 25 µm) showed reduced shear strength at elevated temperature. The thick 120µm bond line specimens showed no significant temperature dependence, illustrating the ability of a thick bond line to both isolate the effect of a large CTE mismatch between die and substrate and reduce the manifestation of thermal stress at the bonding interfaces of the thinner bond line specimens.

Thermal cycling tests showed clear evidence of the detrimental effect that thin bond line, large die area, and large temperature range of operation has on the life and reliability of sintered silver die attachment. The primary failure mechanism was hairline cracks in the bulk of the material at multiple locations and pores coalescing to form wide cracks at the die and/or substrate bonding interface; this was also observed in the bulk of the material in some instances. Unfortunately, SAM images did not give any significant insights into the damage occurring under the die, but die shear tests did give a satisfactory quantitative measure of progressive damage throughout the thermal cycling process. Additionally, the thermal cycling tests provided valuable data that will serve as future validation models for subsequent visco-plastic material model simulations needed for predictive lifing and reliability analyses.

References

[1] Wang,T.; Chen,G.; Wang,Y.; Chen,X.; & Lu,G.Q., “Uniaxial Ratcheting and Fatigue Behaviors of Low-Temperature Sintered Nano-Scale Silver Paste at Room and High Temperatures”, Materials Science and Engineering A, 527 (2010) 6714-6722.

[2] Bai, J.G.; Guo-Quan Lu, "Thermomechanical Reliability of Low-Temperature Sintered Silver Die Attached SiC Power Device Assembly," Device and Materials Reliability, IEEE Transactions, 6-3 (2006) pp.436-441.

[3] Chen, G.; Zhang, Z.S.; Mei, Y.H.; Li, X.; Lu; G.Q; & Chen, X., “Ratcheting behavior of sandwiched assembly joined by sintered nanosilver for power electronics packaging”, Microelectronics Reliability, 53 (2013) 645-651

[4] Kang, G., “A visco-plastic constitutive model for ratcheting of cyclically stable materials and its finite element implementation”, Mechanics of Materials, 36 (2004) 299-312.

[5] Abdel-Karim, M.; Ohno, N., “Kinematic hardening model suitable for ratcheting with steady state”, International Journal of Plasticity, 16 (2000) 225-240.

[6] Bai, J.G.; Yin, J.; Zhang, Z.; Lu, G.Q.; & Van Wyk, J.D., "High-Temperature Operation of SiC Power Devices by Low-Temperature Sintered Silver Die-Attachment", Advanced Packaging, IEEE Transactions, 30-3 (2007) pp.506-510.

[7] Göbl, C.; & Faltenbacher, J., "Low temperature sinter technology die attachment for power electronic applications," Integrated Power Electronics Systems (CIPS), 2010 6th International Conference, (2010) pp.1-5.

[8] Kahler, J.; Heuck, N.; Stranz, A; Waag, A; & Peiner, E., "Pick-and-Place Silver Sintering Die Attach of Small-Area Chips," Components, Packaging and Manufacturing Technology, IEEE Transactions, 2-2 (2012) pp.199-207.

[9] Kisiel, R.; & Szczepański, Z., "Die-attachment solutions for SiC power devices", Microelectronics Reliability, 49-6 (2009) pp. 627-629.

[10] Lei, T.G.; Calata, J.N.; Guo-Quan L.; Xu C.; & Shufang L., "Low-Temperature Sintering of Nanoscale Silver Paste for Attaching Large-Area Chips," Components and Packaging Technologies, IEEE Transactions, 33-1 (2010) pp.98-104.

[11] Li, X.; Chen,G.; Xu,C.; Lu,G.Q.; Wang, L.; & Mei,Y.H., "High temperature ratcheting behavior of nano-silver paste sintered lap shear joint under cyclic shear force", Microelectronics Reliability, 53 (2013) 174-181.

[12] Lu, G.Q.; Calata, J.N.; Lei, G.; & Xu, C., "Low-temperature and Pressureless Sintering Technology for High-performance and High-temperature Interconnection of Semiconductor Devices," Thermal, Mechanical and Multi-Physics Simulation Experiments in Microelectronics and Micro-Systems, 2007. EuroSime International Conference, (2007) pp.1-5.

[13] Lu, G.Q.; Calata, J.N.; Zhiye Z.; & Bai, J.G., "A lead-free, low-temperature sintering die-attach technique for high-performance and high-temperature packaging," High Density Microsystem Design and Packaging and Component Failure Analysis, 2004. HDP '04. Proceeding of the Sixth IEEE CPMT Conference, (2004) pp.42-46.

[15] Zhang, Z.; & Guo-Quan L., "Pressure-assisted low-temperature sintering of silver paste as an alternative die-attach solution to solder reflow," Electronics Packaging Manufacturing, IEEE Transactions, 25-4 (2002) pp.279-283.